Zeitschrift: Schweizerische mineralogische und petrographische Mitteilungen = Bulletin suisse de minéralogie et pétrographie

Band: 76 (1996)

Heft: 2

Artikel: The zeolite, fluorite, quartz assemblage of the fissures at Gibelsbach, Fiesch (Valais, Switzerland) : crystal chemistry, REE patterns, and genetic speculations

Autor: Armbruster, Th. / Kohler, Th. / Meisel, Th.

DOI: https://doi.org/10.5169/seals-57692

SCHWEIZ. MINERAL. PETROGR. MITT. 76, 131–146, 1996

The zeolite, fluorite, quartz assemblage of the fissures at Gibelsbach, Fiesch (Valais, Switzerland): crystal chemistry, REE patterns, and genetic speculations

by *Th. Armbruster*[1], *Th. Kohler*[1], *Th. Meisel*[2], *Th.F. Nägler*[3], *M. A. Götzinger*[4] and *H. A. Stalder*[5]

Abstract

The mineral assemblage quartz, green octahedral fluorite, heulandite, stellerite, epistilbite, laumontite, chabazite, and scolecite occurs in steeply dipping narrow fissures within a M-type granite host rock at Gibelsbach near Fiesch, Valais (Switzerland), located in the southern part of the Aar massif. All fissure minerals were identified by single-crystal X-ray methods and their morphologies were studied by SEM. Electron microprobe analyses indicate that all zeolites represent near Ca end-members. Only heulandite displays a highly significant Sr concentration. Trace elements, including REE, were measured (INAA and IDMS methods) for Gibelsbach fluorite, stellerite and heulandite, rose octahedral fluorite from classic Alpine fissures of the Aar massif, green fluorite from the Säntis area, green fluorite from Hammer (Nufenenpass, Gotthard massif), and from Kleines Furkahorn (Aar massif). REE patterns of whole rock samples surrounding the Gibelsbach occurrence are characteristic of post Archean upper crustal rocks and are significantly different from the flat REE distributions obtained for Gibelsbach fluorite, stellerite, and heulandite. Nd isotopic compositions measured for fluorite and country rock suggest a dominantly crustal origin of the fluid which was subsequently fractionated. The different trace element concentrations in Gibelsbach heulandite and stellerite can be explained by two models: (a) heulandite crystallized from a less fractionated fluid than stellerite and fluorite; (b) the different REE distribution patterns and Sr concentrations are controlled by crystal chemical effects. Interpretation of experimental zeolite stability relations indicates that the Gibelsbach zeolite association formed at peak pressure conditions above 600 bar and temperatures below 230 °C. Laumontite represents the zeolite formed at the highest temperature while chabazite formed at the lowest temperature, probably below 100 °C. Primary fluid inclusions in massive fluorite from Gibelsbach revealed a homogenization temperature of ca. 160 °C and are filled with water low in both salt and CO_2. Thus, the inclusions formed above 200 °C assuming a pressure of ca. 1 kbar based on the geothermal gradient. Steeply dipping fissures in the Aar and Gotthard massif (e.g., at Gibelsbach) are considerably younger (ca. 10 million years old) than the classical Alpine fissures with quartz and rose fluorite (ca. 20 million years old). The youngest relics of hydrothermal activity in the Aar massif are documented by breccia containing opal and chalcedony.

Keywords: fissure minerals, zeolite, fluid inclusion, crystal chemistry, REE, Aar massif, Gibelsbach (Switzerland).

Introduction

A striking zeolite paragenesis occurs at Gibelsbach (altitude 1380 m), north west of the village of Fiesch in Valais, Switzerland. The mineral assemblage was already described by KENNGOTT (1866) to contain green octahedral fluorite, stilbite (synonymous for heulandite at that time), desmine (synonymous for stilbite), small weathered laumontite, and small not well developed adularia (probably confused with epistilbite). The small zeolite outcrop is situated in a strongly foliated

[1] Laboratorium für chemische und mineralogische Kristallographie, Universität Bern, Freiestr. 3, CH-3012 Bern, Switzerland. E-mail: armbruster@krist.unibe.ch.
[2] Department of Geology, University of Maryland, College Park, MD 20742, USA and Laboratorium für Radiochemie, Universität Bern, Freiestr. 3, CH-3012 Bern, Switzerland.
[3] Mineralogisch-petrographisches Institut, Gruppe Isotopengeologie, Erlachstr. 9a, CH-3012 Bern, Switzerland.
[4] Geozentrum, Institut für Mineralogie und Kristallographie, Althanstr. 14, A-1090 Wien, Austria.
[5] Naturhistorisches Museum Bern, Bernastrasse 15, CH-3005 Bern, Switzerland.

M-type granite (KOHLER, 1993). To the north the locality is bordered by a coarse grained granite representing the southern part of the Aar massif (ZBINDEN, 1949). The south border is formed by Permian sedimentary rocks embedded between the Aar- and the Gotthard massif (ZBINDEN, 1949). A detailed description of the Gibelsbach locality is given by KOENIGSBERGER (1940). Many small fissures occur in the strongly foliated M-type granite at a steep wall east of Gibelsbach. The compression or dislocation planes of the host rock dip 50° N. However, most of the small fissures have an inclination of 80° SW. The various fissures and fractures show different mineralizations. Some are completely filled with green fluorite locally covered with zeolites. According to KOENIGSBERGER (1940), the best quality of hand specimens originates from a larger fissure, difficult to access in the steep wall. These samples contain fluorite, heulandite, stellerite (originally described as "Desmin" or stilbite), epistilbite, laumontite, and chabazite.

After more than 150 years of active mineral collecting at Gibelsbach, the outcrop has probably changed its appearance. The steep wall has been extensively exploited and a large scree slope has formed below the original outcrop. Until recently samples from this locality have been sold and exchanged at Swiss mineral fairs. For this reason we mainly rely on the classical description by KOENIGSBERGER (1940). More abundant than fluorite fissures are those only filled with zeolites, either heulandite or stellerite. Such fissures are less than 1 mm wide, but rather laterally extended. In the lower part of the wall typical fissures are 2–10 mm wide and contain short prismatic white quartz often covered with stellerite; in others quartz is covered with fluorite. Fissures containing only quartz are by far most abundant. Further up Gibelsbach, on the west bank of the creek, fissures contain quartz bands with significant amounts of stellerite and occasionally heulandite. Still further up, but within the same host rock, the fissures are covered with thick crusts of stellerite.

The entire occurrence is not consistent with normal Alpine fissures as described by MULLIS (1993) and STALDER (1986). KOENIGSBERGER (1940) concluded that at Gibelsbach fluids invaded from below. This assumption is supported by evidence found at the neighboring Altenbach ca. 250 m above Lax, where a comparable occurrence of fluorite with stilbite (stellerite?) and heulandite was found in a basic rock, differing in composition from the Gibelsbach host rock. PARKER (1973) described a similar zeolite occurrence on the south slope of the Rhone valley 20 km west of Gibelsbach. The Gibelsbach occurrence was classified (PARKER, 1973) as mineral association ("Mineralgesellschaft") A11 which is very heterogeneous but characterized by the predominance of zeolites with additional fluorite. A new locality type (Fundortgruppe 5a) was created for this unique Alpine occurrence (PARKER, 1973). Related to the Gibelsbach mineralization are some quartz occurrences with subordinate fluorite and stilbite (Fundortgruppe 5g) described in the eastern valleys of Valais south of the Rhone river (e.g., Nufenenpass). Quartz in these occurrences is formed in discordant veins (PARKER, 1973).

The goals of this study were to determine the crystal-chemistry of the zeolites from Gibelsbach and to provide a hypothesis of its genesis based on rare earth-element (REE) distributions, fluid inclusions, and zeolite stability. In addition to the Gibelsbach samples, fluorites from other Alpine fissure types were analyzed for comparison.

Mineral identification and analyses

Symmetry and cell dimensions of zeolites were determined from X-ray single-crystal data collected with an Enraf Nonius CAD4 diffractometer using MoKα X-radiation. In addition, single crystals were checked with the polarizing microscope using the oil immersion method.

Carbon-coated polished samples were prepared and analyzed with a CAMECA-SX50-electron microprobe. The electron beam (15 kV, 10 nA) was defocussed to 30 μm in order to minimize sample damage. The following mineral standards were used: orthoclase (Si, Al, K), bytownite (Ca, Na), strontianite (Sr). Results of average analyses are given in table 1. In the observed zeolite association the Si/Al ratio varies between 3.4 (stellerite) to 1.5 (scolecite) but the zeolites with a high Si/Al ratio (stellerite and heulandite) are much more frequent than those with a low Si/Al ratio (chabazite: 2.35, laumontite: 2.0, scolecite: 1.5). The dominant channel cation in all zeolites at Gibelsbach is Ca. Scolecite and laumontite represent nearly Ca end-member composition. Heulandite is the only zeolite which contains major Sr, 11% of the channel cations. In heulandite, stellerite, epistilbite, and chabazite K dominates over Na. The water content was determined by difference. However, due to H_2O loss in the vacuum chamber of the electron microprobe, these H_2O concentrations are considerably lower than the H_2O concentrations of the corresponding zeolites in nature.

To display the morphology of the zeolite minerals, scanning electron micrographs were pro-

Tab. 1 Average electron microprobe analyses for zeolites from the Gibelsbach occurrence at Fiesch. H_2O calculated by difference and formula normalized on O.

wt%	laumontite	heulandite	stellerite	epistilbite	scolecite	chabazite
SiO_2	54.35	60.56	63.57	59.35	46.14	48.03
Al_2O_3	21.48	15.74	15.99	16.59	24.48	17.43
CaO	11.04	6.92	8.53	8.28	13.75	7.09
SrO	n.d.	2.10	0.06	0.14	0.04	0.81
Na_2O	0.02	0.08	0.19	0.35	0.06	0.01
K_2O	1.09	1.53	0.74	1.36	0.01	1.74
H_2O	12.12	13.07	10.92	13.94	15.52	24.89
Si	4.096	24.489	27.700	18.009	24.547	8.473
Al	1.908	8.421	8.211	5.932	15.349	3.623
Ca	0.892	3.365	3.980	2.693	7.835	1.340
Sr	n.d.	0.550	0.015	0.024	0.013	0.082
Na	0.004	0.067	0.164	0.205	0.064	0.005
K	0.105	0.883	0.413	0.527	0.006	0.390
O	12.	72.	72.	48.	80.	24.

duced on samples first impregnated with OsO_4 and then Au-coated.

Solid and fluid inclusions in massive fluorite

Petrographic microscope analyses yielded three types of quartz inclusions in Gibelsbach fluorite (all of similar size 0.05–0.1 mm) : (1) idiomorphic short prismatic quartz, (2) idiomorphic c-axis elongated quartz, (3) broken quartz crystals (mostly of the second type). In addition, flakes of non-specified Ca-rich zeolites were detected with the scanning electron microscope (SEM-EDA).

Four types of fluid inclusions were distinguished in Gibelsbach fluorite: (1) Primary fluid inclusions occurring in the form of small (ca. 5–20 μm) negative tetrahedra containing one liquid (water) and a gas bubble. The ice melting point is near 0 °C (between –1.7 and –0.5 °C) corresponding to a salinity between 1.9 and 0.85 wt% $NaCl_{(equiv.)}$. Homogenization temperatures range from 155 °C to 165 °C (n = 12, x = 158.6 ± 4.0 °C). (2) A few plain inclusions (ca. 25–30 μm in diameter) also contain a single liquid (water) and a gas bubble. The melting point is the same as for type (1): –0.7 °C, and homogenization occurs at 155 °C. (3) Many trails of secondary fluid inclusions cut through some parts of the fluorite. They are generally very small (below 5 μm) and contain mostly one liquid (probably water) and a tiny gas bubble. The ice melting temperature is near 0 °C but the homogenization temperature of one specific population is in the range of 130 °C. (4) Some parts of the fluorites contain completely irregular fluid inclusions forming extended (myrmekitic) water plains. Gas bubbles could not be observed, the melting temperature is at 0 °C.

Trace element determinations

Trace elements including REE and the major elements Na, K, and Ca were determined by instrumental neutron activation analysis (INAA) at the University of Bern for the fluorites F1 to F7, stellerite (S1), heulandite (H1) and whole rock samples TK1 to TK3. Fine powders (20 to 40 mg) were irradiated 1.85 h at a thermal neutron flux of $2 \cdot 10^{13}$ n cm^{-2} s^{-1} in the SAPHIR research reactor of the Paul Scherrer Institute, Würenlingen, Switzerland. Subsequently, γ-spectra were acquired 12 hours, 2–3 days, 1 week, and 3–4 weeks after irradiation. USGS standards BHVO-1 and RGM-1 were used as secondary standards. Fluorite samples NMBE-B8707 and NMBE-B5415 were activated and measured at the Max-Planck-Institut für Chemie at Mainz, Germany. To obtain more precise REE concentrations replicate samples F1 and TK1 were determined by isotope dilution mass spectrometry (IDMS) at the University of Maryland. Precision and reproducibility of these analyses are generally better, 0.5%, corresponding to 2 σ. The analytical technique is described by MEISEL et al. (in review). The analyzed samples are summarized in tables 2 and 3.

Nd isotope ratios were measured at the Isotope Geology Laboratory, Bern, using an AVCO thermal ionization mass spectrometer. Nd ratios were normalized to $^{146}Nd/^{144}Nd = 0.7219$. The mean value for the La Jolla standard during the

Tab. 2 Description of samples used for trace and REE analyses.

No.	**mineral samples**
F1	fluorite Gibelsbach: light green, xenomorphic
F2	fluorite Gibelsbach: colorless octahedra on quartz
F3	fluorite Gibelsbach: dark green, xenomorphic on quartz
F4	fluorite Gibelsbach: colorless octahedra on quartz
H1	heulandite Gibelsbach: grown on quartz
S1	stellerite Gibelsbach: grown on quartz
F5	fluorite Göschenen: rose octahedra
F6	fluorite Säntis: green cubes (KÜRSTEINER and SOOM, 1986)
F7	fluorite Grimsel: rose octahedra
NMBE-B8707	fluorite, Hammer, Nufenenpass: green octahedra (RYKART et al., 1983)
NMBE-B5415	fluorite, Kleines Furkahorn: light green spherulites grown on quartz
	rock samples
TK1	Permian sedimentary rocks embedded between the Aar and Gotthard massif forming the south border of the Gibelsbach locality.
TK2	coarse grained granite characteristic of the southern part of the Aarmassif (ZBINDEN, 1949), northern border of Gibelsbach.
TK3	strongly foliated M-type granite, host rock for the fluorite-zeolite-quartz bearing fissures at the Gibelsbach locality.

period of measurement was 0.51187 $^{143}Nd/^{144}Nd$ with an 2 σ external reproducibility of $\pm$ 0.00002.

Mineralogy and crystal chemistry

Fluorite

The well established structure of fluorite may be described by a simple cubic packing of F where Ca ions occupy the interstices at the center of every other cube leading to eight-fold F coordination of Ca with Ca–F = 2.36 Å. In this structure F is four-fold coordinated by Ca, thus the ionic radius of F becomes 1.31 Å (SHANNON, 1976) and Ca has a radius of 1.05 Å. The origin of color in fluorites has recently been reviewed by LIEBER (1995), who suggests the interaction between γ-radiation and the incorporated foreign elements (e.g., REE) as the major cause of color. The γ-radiation must be produced by the U and Th content of the fluorite itself to cause a homogeneous color distribution in larger crystals (LIEBER, 1995). Colorless and green fluorites from Gibelsbach which occur either as small octahedra or as xenomorphic masses, have approximately 0.5 ppm U and 0.5 ppm Th (Tab. 3). The U and Th concentrations of the host rock are considerably higher, 10 ppm and 13 ppm, respectively. The green fluorite from the Säntis area (F5) has 3.0 ppm U and 2.7 ppm Th, whereas the rose fluorites from the Aar massif have similar U and Th concentrations as the Gibelsbach fluorites. Considering the ionic radii for three-valent REE in eight-fold coordination (1.16 Å for La to 0.977 Å for Lu [SHANNON, 1976]), the observed Ca radius in fluorite falls in the middle of this range. BURT (1989) discusses the substitutional mechanism in fluorite. The simplest way to incorporate REE^{3+} in a Ca-phase is a coupled substitution involving Na: $Na^{+} + REE^{3+} \rightarrow 2\ Ca^{2+}$. Gibelsbach fluorite has 65 to 240 ppm Na, 186 to 765 ppm K, and 60 to 85 ppm REE. However, due to the presence of tiny solid inclusions (mainly quartz and zeolites) it is not clear whether these Na and K concentrations can be assigned to the fluorite itself (GOETZINGER and KOSS, 1995). Another possibility are cation vacancies, thus $2\ REE^{3+} + Vac. \rightarrow 3\ Ca^{2+}$. In addition, anion defects must be considered, in particular interstitial F. BILL and CALAS (1978) also discuss substitutional O^{2-} and charged O molecular complexes.

The term fluorescence is derived from fluorite, where REE characteristic emissions within the optical spectrum are excited by ultraviolet radiation. The fluorescence color is characteristic of the interaction of various REE emission lines (BURRUS et al., 1992). Fluorite from Gibelsbach exhibits intense blue fluorescence under long wave UV radiation.

Stellerite

Stellerite ($Ca_4[Al_8Si_{28}O_{72}] \cdot 28\ H_2O$), stilbite ($NaCa_4[Al_9Si_{27}O_{72}] \cdot 30\ H_2O$, and barrerite ($Na_8[Al_8Si_{28}O_{72}] \cdot 26\ H_2O$) possess the same tetrahe-

Tab. 3 Trace element analyses of selected rock (TK1–TK3) and mineral samples. Underlined concentrations are in wt% all others are in ppm. Sample descriptions are given in table 2.

	country rock			fluorites Gibelsbach				fluorites other localities					zeolites		
ppm	TK1	TK2	TK3	F1	F2	F3	F4	F5	F6	F7	B8707	B5415	H1	S1	error
Na	2.20	2.69	2.64	65	82	70	242	17	32	75	36.9	103	849	1676	5%
K	0.72	2.81	2.47	186	203	765	571	45	37	89	29	601	1.74	0.92	3%
Ca	5.3		1.9	53.7	44.6	42.7	52.7	57.8	56.1	52.6	51.3	38.0	5.2	9.8	9%
Sc	7.1	10.4	8.1	0.2	0.03	0.1	0.2	0.01	0.1	0.1	0.052	0.087	0.2	0.1	8%
Cr	46	2.6	3.0	1.7	13.1	0.7	1.9	0.3	0.6	< 0.1	3.1	2.5	12.6	2.5	10%
Mn	1407	894		4	3	3	8	0.4	0.3	4	1.5	5.8	172	29	3%
Fe	2.23	2.65	2.05	0.02		0.02	0.03	0.01		0.02	0.003	0.047	0.10	0.04	6%
Co	44	34	30	0.1		0.1	0.1	0.1	0.05	20.9	0.13	0.4	3.4	0.2	10%
Zn	41	38	32	0.4		3	3	1	0.2	3	18	3.1	17	8	10%
Ga	10	17				0.3	0.4			0.1	< 0.04	0.5	3	2	10%
Rb	45	171	169			6					< 0.5	5.4	32	9	9%
Sr		196		149		96	164	69	173	222	72	124	18300	280	12%
Zr		141	346	56		31	54		20		< 5	< 10		4	16%
Cs	4.3	6.1	3.0	0.2		0.3	0.5				0.02	0.16	9.0	0.9	25%
Ba	494	575	591	19							< 5	7.6	143	22	20%
La	22.0	35.1	13.1	7.2	6.4	6.3	9.5	0.05	3.3	0.3	5.2	13.5	1.9	0.6	9%
Ce	44.3	74	27	*13.1*	12	12	17	0.17	9	1	12.5	25.1	6	1	9%
Pr											1.7	2.7			15%
Nd	*20.5*	34	15	13	10	11	17		9		7.7	9.9	2	1	11%
Sm	*4.25*	6.0	3.2	*6.08*	5.1	4.2	5.6	0.06	3.8	0.6	4.61	1.96	0.20	0.36	7%
Eu	*0.85*	0.78	0.76	*2.69*	3.22	1.67	2.16	0.04	0.72	0.31	1.07	0.86	0.06	0.17	7%
Gd	*4.04*	6.5		*10.8*	4.1	4.6	5.1	0.4	5.8	4.0	8.3	3.5	0.20	0.40	39%
Tb	0.41	0.80	0.66	1.57	1.0	0.84	1.01	0.21	1.04	0.7	1.62	0.37	0.03	0.07	15%
Dy	*3.52*			*9.29*		6.9	7.7	5.1	7.4		8.86	2.07			3%
Ho			1.17	2.6	0.74	1.4	1.9	2.4	1.7	2.0	1.7	0.4			25%
Er	*2.19*			*6.91*		4.0	5.7	11.6	3.6		4	1.02			10%
Tm		0.55	0.61	0.27	0.36	0.15	0.20	0.28	0.11	0.42	0.54	0.17		0.04	16%
Yb	*2.27*	3.7	3.6	*7.90*	4.4	4.4	8.0	12.3	1.6	8.8	3.09	0.77	0.1	0.5	13%
Lu	0.33	0.65	0.56	1.95	1.09	0.83	1.72	1.95	0.18	1.85	0.36	0.11	0.03	0.11	9%
Hf	3.2	4.5	4.4			0.05	0.05	4.3			< 0.02	0.04	0.11		15%
Ta	2.1	3.1		0.22			0.08	0.43		0.66	< 0.015	0.008	0.49	0.03	20%
Th	6.1	19.0	13.3	0.19	0.3	0.56	0.40	0.04	2.74	0.16	0.14	0.11	1.99	0.53	10%
U	2.2	6.8	9.8	0.45	0.8	0.39	0.64		2.97	0.75	0.06	1.17	1.02	0.51	15%

dral framework structure and are distinguished by 2 Na → Ca substitution and different H_2O content (GOTTARDI and GALLI, 1985). These minerals have large channels (4.9 × 6.1 Å) parallel to [100] formed by ten-membered rings of tetrahedra. The channels are further connected through windows formed by eight-membered rings along [102], 5.6 × 2.7 Å wide and along [001], 4.0 × 2.7 Å wide (MEIER and OLSON, 1992).

Stellerite from Gibelsbach (identical to "Desmin" in PARKER, 1973) forms white radiating bundles of elongated crystals up to 20 mm in length. This mineral has only a very low Na concentration (0.16 p.f.u. based on 72 O) but 0.41 K p.f.u., which is rather high. Most stilbites (space group *C2/m*) have a composition close to $NaCa_4(Al_9Si_{27}O_{72}) \cdot 30\ H_2O$ were Na can reach up to 2.58 p.f.u.; a K analog is not known. In contrast to stilbite, stellerite is orthorhombic (space group *Fmmm*) and untwinned. Both minerals (stilbite and stellerite) have a disordered Si,Al distribution (GALLI and ALBERTI, 1975). The lower symmetry of stilbite is caused by the close proximity of Na and Ca positions within the crystal structure, thus Ca is shifted from the (010) mirror plane in an ordered fashion leading to monoclinic symmetry (GOTTARDI, 1979). Stellerite from Gibelsbach has orthorhombic cell dimensions a = 13.589(5), b = 18.17(1), c = 17.789(3) Å with no indication of twinning as analyzed by single-crystal X-ray methods and crystal optics. The morphology (Fig. 1) is characterized by well developed {100}, {010}, and {111} faces with an additional small {001} face. "Desmin" from Gibelsbach should actually be considered a K-rich stellerite. The first published analysis of Gibelsbach "Desmin" by Jakob (NIGGLI, 1940) indicated very low Na and K concentrations characteristic of stellerite. These findings are in good agreement with X-ray and chemical data given by PASSAGLIA

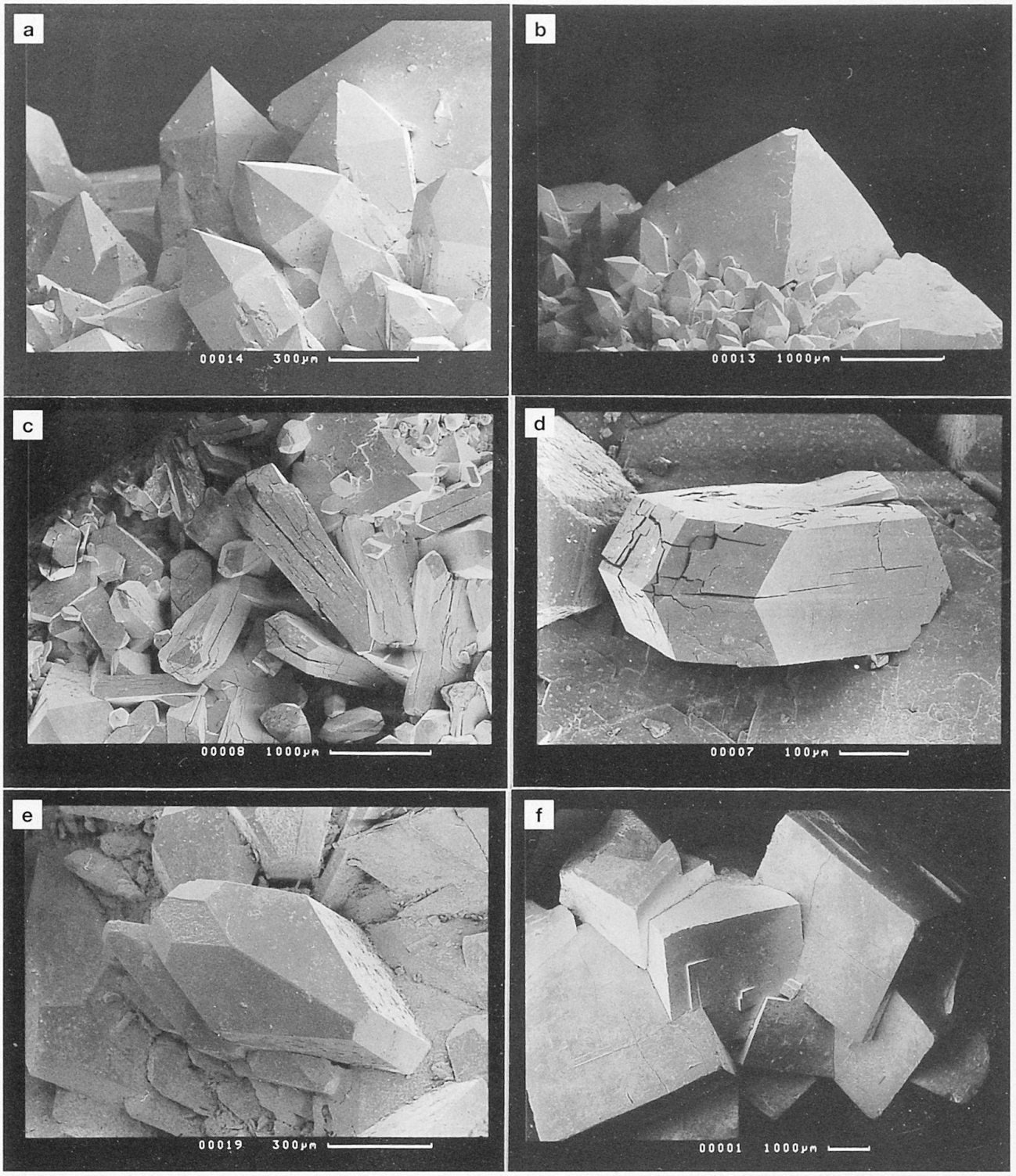

Fig. 1 Scanning electron microscopic images of selected fissure minerals from Gibelsbach (courtesy of F. Zweili, Bern).
(a) small short prismatic quartz representing the dominant fissure mineral;
(b) green octahedra of fluorite frequently overgrowing quartz;
(c) stellerite forms bundles or intergrowths of elongated crystals, the cracks probably developed because of the vacuum in the scanning electron microscope;
(d) characteristic stellerite single-crystal;
(e) characteristic epistilbite twin, the (100) twin plane runs through the ridge of the crystal, the ($\bar{1}02$) face on the top is strikingly rough on all crystals;
(f) intergrown clusters of chabazite rhombohedra (pseudocubes);

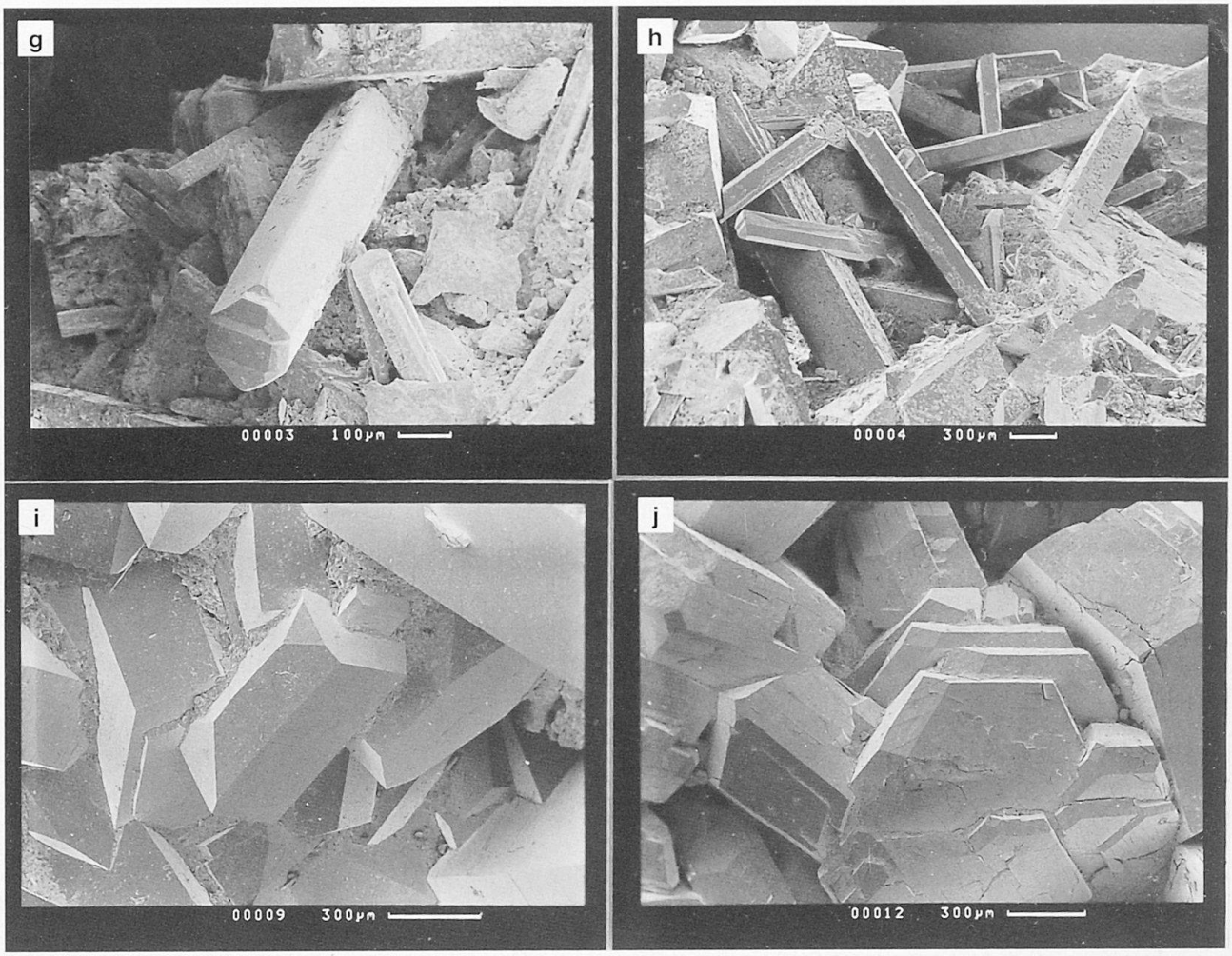

(g) fibrous twinned scolecite with complex termination;
(h) clusters of scolecite;
(i) blocky heulandite;
(j) stacks of flattened heulandites.

et al. (1978) for stellerite from the same locality (their sample #14). These authors did not observe splitting of the 204 powder X-ray diffraction peak which, if present, would indicate deviation from orthorhombic symmetry.

Epistilbite

Epistilbite, space group *C2* (ALBERTI et al., 1985), is structurally not related to stilbite (GOTTARDI and GALLI, 1985) but was named epistilbite because of its similarity to stilbite (ROSE, 1826). Epistilbite, with a disordered Si,Al distribution, possesses structural channels parallel [001] formed by eight-membered rings of tetrahedra, ca. 3.7 × 5.2 Å wide, connected along [100] by windows formed by ten-membered rings, 3.4 × 5.6 Å wide (MEIER and OLSON, 1992). Epistilbite from Gibelsbach $Ca_{2.7}Na_{0.2}K_{0.5}(Al_{5.9}Si_{18.0}O_{48}) \cdot 16\ H_2O$ deviates slightly from the mean formula $Ca_{2.5}Na_{0.8}K_{0.2}(Al_6Si_{18}O_{48}) \cdot 16\ H_2O$ (GALLI and RINALDI, 1974) mainly because the concentration of K is higher than Na. Single-crystal X-ray intensities of reflections hkl and h–kl should be equal in a monoclinic space group, which is not the case for several weak and medium intensity reflections of Gibelsbach epistilbite, thus triclinic symmetry (*C1*) as proposed by AKIZUKI and NISHIDO (1988) must be suspected (YANG and ARMBRUSTER, 1996). The cell dimensions are a = 9.082(1), b = 17.738(3), c = 10.209(1) Å, α = 89.95(1), β = 124.57(1), γ = 90.00(1)°. Epistilbite from Gibelsbach is white-cream in color and up to 4 mm in length. This mineral cannot be mistaken for stilbite because of its unique morphology at this locality (Fig. 1). As known for all other epistilbite occurrences, the crystals are characterized by (100) twins, but this mineral has no tendency to form bundles as does stilbite. Idiomorphic crystals

are terminated by {110}, {1$\bar{1}$0}, {010}, {0$\bar{1}$0}, {012}, {0$\bar{1}$2}, and by small but strikingly rough {$\bar{1}$02} faces.

Heulandite

The heulandite group of minerals is represented by heulandite $(Na,K)Ca_4(Al_9Si_{27}O_{72}) \cdot 24\ H_2O$ and clinoptilolite $(Na,K)_6(Al_6Si_{30}O_{72}) \cdot 20\ H_2O$ (GOTTARDI and GALLI, 1985). The crystal structure is characterized by dense tetrahedral layers parallel to (010) with channels formed by ten-membered rings (A) and eight-membered rings (B) running parallel to [001] which are interconnected by additional channels (C) formed by eight-membered rings along [100] and [102] leading to a two-dimensional channel system. Heulandite from Gibelsbach has the composition $Na_{0.07}K_{0.88}Ca_{3.37}Sr_{0.55}(Al_{8.42}Si_{27.49}O_{72}) \cdot 24\ H_2O$ and occurs either in tabular habit (TSCHERNICH, 1992) elongated along the **a**-axis and highly flattened on {010} or in blocky habit (Fig. 1). MERKLE and SLAUGHTER (1968) assumed *Cm* space group symmetry for Gibelsbach heulandite. However, structure refinements carried out in this study show no significant deviation from space group *C2/m* with the cell dimensions $a = 17.705(3)$, $b = 17.890(2)$, $c = 7.419(2)$ Å, ß = 116.53(2)°.

Chabazite

Chabazite has a channel system formed by eight-membered rings of tetrahedra, 3.8 × 3.8 Å wide (MEIER and OLSON, 1992) and an ideal composition of $Ca(Al_4Si_8O_{24}) \cdot 12\ H_2O$ (GOTTARDI and GALLI, 1985). Chabazite from Gibelsbach has the composition $K_{0.39}Ca_{1.34}Sr_{0.08}(Al_{3.62}Si_{8.47}O_{24}) \cdot 12\ H_2O$ and occurs in simple transparent pseudocubic rhombohedra without striations, 0.3 to 20 mm across. Very often the rhombohedra are intergrown into clusters (Fig. 1). With the polarizing microscope using crossed polarizers Gibelsbach chabazite exhibits undulatory extinction. According to AKIZUKI (1981) the optical properties correspond to the degree of Si,Al ordering which differs from growth sector to growth sector. Thus, chabazite showing rhombohedral forms consists of six twinned sectors. Early structure refinements of chabazite discussed by GOTTARDI and GALLI (1985) were performed in the rhombohedral space group $R\bar{3}m$ which is the maximum symmetry compatible with the framework. MAZZI and GALLI (1983) separated domains from well developed chabazite twins and found significant deviations from trigonal symmetry leading to space group $P\bar{1}$. In agreement with the optical studies by AKIZUKI (1981) the lower symmetry is caused by partial Si,Al ordering. All X-ray single-crystal reflections of Gibelsbach chabazite are extremely sharp in the ω direction which is rather unusual for a supposed twin. In addition, cell dimensions refined from single-crystal data do not significantly deviate from rhombohedral symmetry ($\alpha_{rh} = 9.389(1)$ Å, $\alpha_{rh} = 94.25(2)°$; $a_h = 13.774(2)$, $c_h = 15.027(5)$ Å). Thus, it is very unlikely that chabazite from Gibelsbach consists of microscopic twins.

Scolecite

Scolecite, ideally $Ca_8(Al_{16}Si_{24}O_{80}) \cdot 24\ H_2O$, represents the only fibrous zeolite found at Gibelsbach. The same structural framework is also found for natrolite $Na_{16}(Al_{16}Si_{24}O_{80}) \cdot 16\ H_2O$ and mesolite $Na_{16}Ca_{16}(Al_{48}Si_{72}O_{240}) \cdot 64\ H_2O$. Minerals of this group are distinguished by a $Ca + H_2O \rightarrow 2\ Na$ substitution and symmetry (GOTTARDI and GALLI, 1985). Electron microprobe analyses of Gibelsbach scolecite yielded the formula $Na_{0.06}Ca_{7.84}(Al_{15.35}Si_{24.55}O_{80}) \cdot x\ H_2O$. Scolecite from Gibelsbach (space group *F1d1*, cell dimensions: $a = 18.58(4)$, $b = 18.91(4)$, $c = 6.57(2)$ Å, β = 90.7(3)) was often mistaken for laumontite, however, the shiny luster of the strongly fibrous crystals makes this confusion inconceivable. Scolecite from near Fiesch was previously described by HINTZE (1897). However, this occurrence is at the Fiesch glacier (WISER, 1860). To our knowledge, scolecite from Gibelsbach has not been described. The habit of Gibelsbach scolecite (Fig. 1) is characterized by (100) twins leading to a "complex termination" (TSCHERNICH, 1992; Fig. 523).

Laumontite

Laumontite with the ideal composition $Ca_4(Al_8Si_{16}O_{48}) \cdot 18\ H_2O$ (ARMBRUSTER and KOHLER, 1992) and space group *C2/m* has a completely ordered Si,Al distribution and one dimensional structural channels running parallel to the c-axis confined by ten-membered rings of tetrahedra. When removed from the humidity of the fissure, laumontite spontaneously dehydrates to form the variety leonhardite, $Ca_4(Al_8Si_{16}O_{48}) \cdot 14\ H_2O$, which becomes milky white and is extremely fragile. Cell dimensions collected on natural laumontite are therefore always characteristic of the partially dehydrated variety. At Gibelsbach, laumontite has the composition $Ca_{3.56}K_{0.44}(Al_{7.64}Si_{16.40}O_{48}) \cdot x\ H_2O$. Laumontite crystallizes in characteristic stalks up to 5 mm long formed by {110} and {001} faces. Laumontite from Gibelsbach was described by KENNGOTT (1866) as very small weathered crystals. Due to the strong tendency to disintegrate, it is difficult to estimate the true frequency of this mineral in the exposed fissures.

REE patterns

The results of INAA and IDMS are shown in chondrite normalized plots (Fig. 2) using the values for Leedy (MASUDA et al., 1973). In these diagrams the La and Tb values of INAA are used to complete the ID-MS pattern for sample F1 (light green fluorite from Gibelsbach). All analyzed fluorites from Gibelsbach are characterized by more or less flat REE distributions (Fig. 2e). Slightly negative anomalies for Ce are common for these fluorites. A positive Eu anomaly (Eu/Eu* > 1) is only significant for sample F2. The heavy REE show a flat distribution or a slight positive trend. Fluorite F1 has a high Sm/Nd ratio (0.442). If this is taken as representative of the source, the latter would have to be highly LREE depleted. Sources of that kind (i.e., depleted mantle or mafic to ultramafic rocks from the depleted mantle) are, however, also characterized by strongly positive ε_{Nd} values (ε_{Nd} values express the Nd isotopic composition as deviation from coeval bulk earth

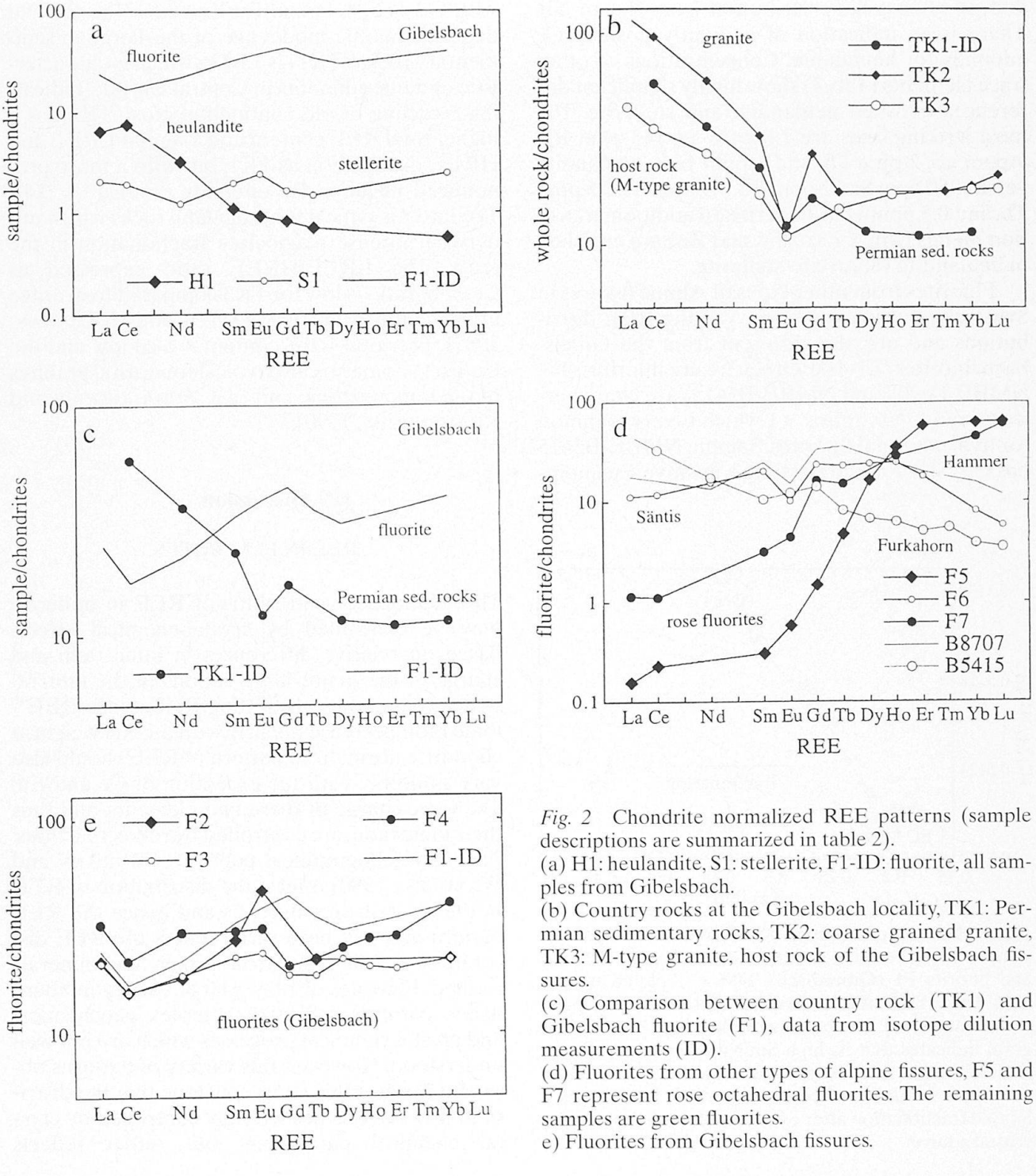

Fig. 2 Chondrite normalized REE patterns (sample descriptions are summarized in table 2).
(a) H1: heulandite, S1: stellerite, F1-ID: fluorite, all samples from Gibelsbach.
(b) Country rocks at the Gibelsbach locality, TK1: Permian sedimentary rocks, TK2: coarse grained granite, TK3: M-type granite, host rock of the Gibelsbach fissures.
(c) Comparison between country rock (TK1) and Gibelsbach fluorite (F1), data from isotope dilution measurements (ID).
(d) Fluorites from other types of alpine fissures, F5 and F7 represent rose octahedral fluorites. The remaining samples are green fluorites.
e) Fluorites from Gibelsbach fissures.

in parts per 10^4). The negative ε_{Nd} value of fluorite F1 (–4.3) is indicative for a dominantly crustal origin. Consequently, the high Sm/Nd ratio of 0.442 of the fluorite must be interpreted as unrelated to the source (i.e., as later fractionation [Fig. 3]).

The zeolite samples are characterized by an overall lower REE abundance (Fig. 2a) but normalized to Ca the concentrations are comparable to the fluorites. Stellerite has a pattern similar to the fluorites but without the negative Ce anomaly. Heulandite is characterized by LREE > HREE and an almost flat distribution from Sm to Yb. There is an indication of a slightly positive Ce anomaly for heulandite. Concentrations of other trace elements (Tab. 3) show highly significant differences between heulandite and stellerite. The most striking ones are 1.8 wt% Sr, 143 ppm Ba, 9 ppm Cs, 2 ppm Th, and 1 ppm U in heulandite versus 250 ppm Sr, 22 ppm Ba, 0.9 ppm Cs, 0.5 ppm Th, and 0.5 ppm U in stellerite. In addition, transition metals (Mn, Cr, Co, Fe, and Zn) are enriched in heulandite relative to stellerite.

Fluorites from other types of Alpine fissures in Switzerland display strongly varying REE distributions and are also different from the Gibelsbach fluorites (F1–F4). Green fissure fluorites (F6, NMBE-B8707 and NMBE-B5415) are characterized by Gd_n/Yb_n ratios > 1 which is very common for hydrothermal fluorites. Sample NMBE-B5415 has $Ce_n/Sm_n > 1$ and possibly a positive Eu anomaly, whereas F6 and NMBE-B8707 have negative Eu anomalies and a Ce_n/Sm_n ratio < 1 which is also widely observed for fluorites. The fissure rose fluorites F5 (Göschenen) and F7 (Grimsel) are very unusual with very small Ce/Yb ratios. Sample F5 has the lowest Ce concentration but the highest Yb value of all samples analyzed.

The three country rock samples have overall pattern typical for post Archean upper crustal rocks with LREE > HREE and negative Eu anomalies. TK1 has characteristics of typical post Archean shales (TAYLOR and MCLENNAN, 1985) with Gd_n/Yb_n 1.44 and Eu/Eu* 0.63. The Sm–Nd depleted mantle model age of the Permian sedimentary rocks (TK1) is 1.8 Ga which is characteristic of metasediments in Central Europe, indicating recycling of old continental crust. TK2 has a higher total REE content and a similar LREE and HREE distribution as TK1, but with a more pronounced negative Eu anomaly (Eu/Eu* = 0.4). The latter is typical for magmatic rocks which underwent intense plagioclase fractionation in the crust. The LREE/HREE ratio expressed as Ce_n/Yb_n ratio is low for TK3 compared to average upper continental crust (TAYLOR and MCLENNAN, 1985). The total REE content is also low and the Eu/Eu* anomaly is also typical for crustal granites of the same tectonic unit (e.g., SCHALTEGGER and KRÄHENBÜHL, 1990).

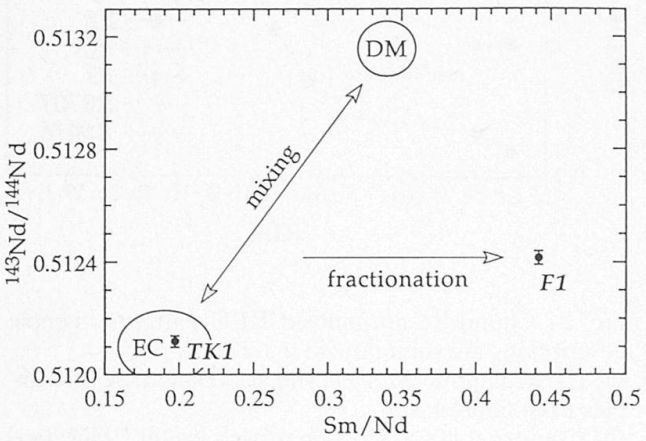

Fig. 3 Nd isotopic composition versus Sm/Nd ratios of sample TK1 (Permian sedimentary rocks, Gibelsbach) and fluorite F1 (Gibelsbach). DM = depleted mantle field, EC = field of compositions typical for European continental crust. The position of fluorite F1 in this diagram indicates that its high Sm/Nd ratio cannot be inherited from a mantle type source, a continental crust source, or a mixing of both. In contrast it indicates a Sm/Nd fractionation after extraction from a dominantly crustal source.

Discussion

REE IN FLUORITES

The abundances and ratios of REE in minerals may be controlled by crystal-chemical effects based on relative differences in ionic radii and charge of the major large cations in the mineral structure and the substituting REE. Since REE^{3+} ionic radii decrease linearly with atomic weight, a chondrite normalized pattern of REE should also vary smoothly with the exception of Ce and Eu. The ionic charge of these two elements, and thus their ionic radii, are controlled by redox reactions. The "crystallographical control" (MORGAN and WANDLESS, 1980) affects the distribution of REE in the crystallizing minerals and hence the REE pattern may not necessarily reflect the REE distribution in the fluid from which the minerals formed. Fluorites display a large variety in abundance patterns reflecting complex geochemical and crystal chemical processes which are not well understood. However, this variety of patterns observed for fluorites let us conclude that the distribution of REE is not strongly controlled by crystal chemical parameters but rather reflects

processes controlling the composition of the fluid. An exception must be stated if the REE reservoir where CaF_2 precipitates is finite (MARCHAND et al., 1976). In this case the solution will gradually be enriched in LREE.

Several authors have tried to ascribe the shape of REE patterns to processes related to the temperature of formation which controls the stability of REE complexes in solution. It is believed that $La_n/Yb_n > 1$ (Tb/La low) reflect crystallization of fluorite at an early stage whereas $La_n/Yb_n < 1$ (Tb/La high) should represent fluorites which crystallized at a late stage when LREE have already been depleted in the solution (MOELLER et al., 1976). Empirical data from LEEDER (1966) and FLEISCHER (1969) demonstrate that uptake of REE into the fluorite lattice is optimum in the region of Tb–Ho. Samples NMBE-B8707 and F6 are indeed humped in shape with a maximum in the chondrite normalized patterns in this range. Similar patterns have been described by BAU and DULSKI (1995), CHESLEY et al. (1994), and EKAMBARAM et al. (1986). Although these distributions seem to be very common, the existence of abundance patterns which are very different suggests a combination of different controlling processes. The stability of monofluoro REE complexes increases smoothly from La to Lu (WALKER and CHOPPIN, 1967). Carbonate-REE complexes, although not as stable as REE-F complexes, might also control the abundance seen in fluorites. This leaves us with too many unknown parameters. Thus, making an accurate evaluation of formation processes is very speculative. An additional problem arises because Sm/Nd ratios and thus REE patterns have been significantly altered through fluorite recrystallization at least under greenschist facies (or higher) conditions (NÄGLER et al., 1995).

COLOR, AND MORPHOLOGY OF FLUORITES FROM ALPINE FISSURES

Rose colored fluorites with octahedral forms (F5 and F7) from Alpine fissures of the Aar massif have strongly enriched HREE (chondrite normalization) relative to the other fluorites. This pattern is commonly explained by the primary crystallization of LREE-rich minerals such as monazite, epidote, allanite, titanite, crichtonite, davidite, and perovskite. The REE pattern of octahedral rose fluorite (this study) differs from the surrounding host rocks which have LREE enriched and a strongly negative Eu anomaly (SCHALTEGGER and KRÄHENBÜHL, 1990). The low LREE/HREE ratios seem to be a common feature for all Alpine rose fluorites as indicated by various other studies (e.g., SPETTEL et al., 1981). STALDER (1985) estimated that quartz in the fissure Gerstenegg (Grimsel, Aar massif) associated with quartz, chlorite, octahedral rose fluorite, and calcite was formed at approximately 430 °C and 2.8 kbar. Slightly lower formation conditions must be assumed for the growth of rose fluorite, as this mineral crystallized after quartz.

The origin of the rose color in fluorite was studied by BILL et al. (1967), BILL and CALAS (1978), and TRINKLER et al. (1993). The color originates from a 485 nm absorption band attributed to a YO_2 color center. Y^{3+} has a ionic radius of 1.019 Å (SHANNON, 1976) and behaves geochemically similar to HREE with corresponding ionic radii. In addition, a weak absorption at 365 nm is assigned to optically active Yb^{2+}. There seems to be a strong correlation between growth conditions and formations of specific types of color centers. The fissures bearing octahedral rose fluorite in the Aar massif represent the oldest fluorite bearing fissures which also formed at the highest temperature.

The green color of fluorite (from Dürrschrennenhöhle, Säntis, Switzerland, sample F6) was assigned to a Sm^{2+} color center which disappears upon heating above 300 °C where Sm^{2+} is oxidized to Sm^{3+} (BILL et al., 1967). This Säntis fluorite for which KÜRSTEINER and SOOM (1986) assume crystallization together with quartz and calcite at approximately 160 °C, has REE enriched by a factor of 10 times chondrite. A very similar REE pattern and enrichment is observed for fluorite from Hammer (Nufenenpass, Gotthard massif; sample NMBE-B8707). At the Hammer locality octahedra prevail cubeoctahedral forms (RYKART et al., 1983) whereas at Säntis cubes and rhombic dodecahedra are more common than octahedral forms (KÜRSTEINER and SOOM, 1986; PARKER, 1973). All green fissure fluorites from the Aar or Gotthard massif, including those from Gibelsbach (Tab. 2: samples F1, F3, NMBE-B8707, NMBE-B5415) have much less fractioned REE patterns compared to the rose ones (F5, F7). For the Gibelsbach samples there is no direct correlation between REE or Sm concentration (Tab. 3) and green color intensity confirming observations by MARCHAND et al. (1976).

Parageneses and crystal forms of fluorites were compared and discussed by OBENAUER (1933). Octahedral fluorites seem to represent the first generation in pneumatolytic formations. However, no direct correlation between fluorite crystal form and fluid temperature, acidity, and composition could be shown. Nevertheless, it is well established from field evidence that fluorite

formed at low temperature crystallizes in cubes (e.g., GOETZINGER and WEINKE, 1984; VON FELLENBERG, 1891).

REE IN ZEOLITES

Several factors are responsible for the exchangeability of cations in zeolites: the charge of the cation controls the Coulomb-type interaction with the framework; the Al concentration in the framework leads to negative charges on the cavity walls; the order-disorder distribution of Si and Al in the framework governs most probable cation positions within the structural channels and the size of the cation, including its hydration sphere, relative to the size of the cavities and windows influences the mobility of the ion or complex within the structural channels. The three-valent charge and the radius varying between 1.18 Å (La^{3+}) and 0.97 Å (Lu^{3+}) in eight-fold oxygen coordination, imply relatively stable incorporation of REE in zeolite channel systems. The smallest channel inlets or outlets in heulandite and stellerite are formed by eight-membered rings of tetrahedra and both minerals have very similar Al concentrations which display a high degree of disorder. Thus, from a crystal chemical point of view stellerite and heulandite may have very similar affinity to REE.

The REE abundance pattern of stellerite is very similar to fluorite F1: a maximum in the MREE (Sm–Gd) and $Dy_n/Yb_n < 1$. If we consider analytical error, the LREE patterns are also similar. Provided that crystal chemical parameters do not control the REE abundance then the similarity in overall patterns indicates (simultaneous) coeval crystal formation. If the same hold true for the heulandite sample, then its crystallization preceded fluorite and stellerite. Or more cautiously, the fluid producing heulandite was less REE differentiated compared to the one producing stellerite and fluorite. In hand specimen, stellerite often grows on fluorite whereas the majority of heulandite grows on quartz. In particular, the heulandite investigated for REE in this study did not grow on fluorite. Furthermore, we must consider the high Sr concentration in heulandite in contrast to stellerite as characteristic for this locality (e.g., MERKLE and SLAUGHTER, 1968; electron microprobe analyses [this paper]; and trace element determinations [this paper]). This, and the difference in concentrations of other trace elements, may be additional indications that different fluids produced stellerite and heulandite. Both stellerite and fluorite have a common low Sr concentration.

Nevertheless, a crystal chemical control of the REE distribution in heulandite and stellerite cannot be completely excluded. Even if the smallest channel inlets or outlets are formed by eight-membered rings of tetrahedra, the different shape of these rings in the two structures may cause largely different crystal chemical behavior. The increased concentration of LREE (with large ionic radii) in heulandite relative to stellerite (Tab. 3) could indicate a crystal chemical preference. The preference of Sr (ionic radius: 1.25 Å, to compare with the one of La^{3+} of 1.18 Å) in heulandite (Tab. 3) even favours this interpretation.

Eu AND Ce ANOMALIES

Since the extent of Eu/Eu* anomalies shows a large range in fluorites, we assume that the abundance is not controlled by the size of the atom relative to the crystal lattice but rather reflects the composition of the solution. Whereas the majority of REE have 3+ as normal oxidation state, europium can occur in two oxidation states (Eu^{2+} and Eu^{3+}). Under low oxygen fugacities Eu^{3+} (1.03 Å) will be reduced to Eu^{2+} having a larger ionic radius (1.12 Å). The four fluorites from Gibelsbach are LREE depleted and have no, or positive, Eu anomalies (Eu/Eu* > 1). This indicates that the reducing condition did not occur during or before fluorite crystallization which is consistent with negative Ce anomalies occurring under high oxygen fugacity. Under oxidizing condition Ce will form Ce^{4+} and will precipitate as CeO_2 depleting the solution in Ce relative to La and Pr.

As stated in the results section (REE patterns) the Nd isotopic composition of fluorite F1 (ε_{Nd} = –4.3) indicates that Nd dominantly originates from a continental crust source (i.e., a source with an enriched LREE pattern). The depleted patterns of Gibelsbach fluorite can be explained by removal of LREE prior to crystallization. This seems to be a common principle as observed by CONSTANTOPOULOS (1988). If REE with larger ionic radii and thus lower stability of fluoride complexes are removed at early stages of fluorite formation, Eu^{2+} will also be depleted relative to Sm and Gd. This could be true for most of the fluorites reported in the literature. CONSTANTOPOULOS (1988) reports three fluorites from one district with Ce_n/Yb_n and Eu/Eu* > 1. If these fluorites formed at an early stage, then the hypothesis of early removal and enrichment of LREE and Eu^{2+} is valid and subsequently crystallized fluorites must also be depleted in these elements. A slightly positive Ce anomaly and no Eu anomaly is con-

sistent with formation of heulandite prior to fluorite and stellerite, removing Ce and LREE.

GENETIC SPECULATIONS

Alpine fissures in the Aar and Gotthard massif

Two characteristic morphological forms of classical Alpine fissures are distinguished (MULLIS et al., 1994): (a) tension gashes usually developed parallel to the maximum stress and perpendicular to the maximum elongation and (b) interboudin gaps developed parallel to the direction of maximum extension in rocks of different competence. These oldest fissures in the Aar and Gotthard massif must have opened around 20 and 15 million years ago as a consequence of late stage continental collision between Europe and Africa (MULLIS et al., 1994). At Grimsel (Aar massif) the oldest fissures (ca. 20 million years old), type 1, are characterized by smoky quartz and octahedral rose fluorite. The hydrous fluid inclusions in quartz are salt-rich but CO_2-poor. Younger fissures (ca. 15 million years old), type 2, have no smoky quartz or fluorite and the hydrous fluid inclusions in quartz are salt-rich and CO_2-bearing.

A still younger generation of narrow fissures (type 3) was described by OGI and SOOM (1988) from Eggerberg (Aar massif). These narrow fissures are inclined to the host rock schistosity and bear light green fluorite which appears macroscopically as rhombic dodecahedra. Microscopically the crystal surface is build by {100} steps.

Still younger are extended nearly vertical fissure systems (type 4) bearing predominantly quartz with subordinate fluorite and occasionally zeolites (e.g., Nufenen pass area [RYKART et al., 1983; PARKER, 1973; sample NMBE-B8707, this study], and Gibelsbach [this study]). STALDER et al. (1980) and POTY et al. (1974) report CO_2- and salt-poor hydrous fluid inclusions in quartz for these vertical fissures which agrees with the findings from Gibelsbach.

At Kleines Furkahorn (Aar massif) quartz in a normal mineralized fissure is overgrown by younger light greenish fluorite (type 5) forming half-spheres of intergrown aggregates (sample NMBE-B5415, this study).

The youngest evidence of hydrothermal activity (type 6) in the Aar massif is the breccia at Trübtensee where chalcedony is found as matrix (STALDER, 1964; DOLLINGER, 1989). In addition, RYKART and HOTZ (1987) report young opal formations ("hyalite") in considerably older fissures with primary quartz, calcite, albite, adularia, titanite, epidote, and chlorite, occurring in biotite rich schists in the northern part of the Aar massif (near Guttannen). These young opal ("hyalite") formations in the Aar massif are not unique but have also been observed at other localities. The temperature-age relations of hydrothermal activities and fissure formation in the Aar massif are displayed in figure. 4.

The Gibelsbach occurrence

Considering equilibrium stability relations of various Ca dominant zeolites as experimentally determined by CHO et al. (1987), one should assume that the peak pressure conditions at Gibelsbach were above 600 bar. Above this pressure and above ca. 130 °C heulandite fills a gap in the P-T field between stilbite (actually stellerite) which forms at lower temperatures and laumontite which forms at higher temperatures. At 600 bar, laumontite remains stable up to ca. 230 °C where it transforms to wairakite (not observed at Gibelsbach and also never described from the Swiss Alps). However, these stability relations are only valid in the simple system $CaAl_2Si_2O_8$–SiO_2–H_2O (CHO et al., 1987) where $P(H_2O) = P(total)$ which is unlikely in fissure systems. On the other hand, if we consider zeolite formation in the geothermal areas of Iceland (KRISTMANNSDOTTIR and TOMASSON, 1978) heulandite formed also at shallow depth (< 300 m); thus, elevated pressures seem not to be requisite for heulandite formation. At Iceland where the temperatures in the drill hole were measured directly, chabazite was found below 70 °C, scolecite between ca. 70 and 100 °C, stilbite, epistilbite and heulandite between ca. 70 and 150 °C, and laumontite above 100 °C up to 230 °C (KRISTMANNSDOTTIR and TOMASSON, 1978).

At Gibelsbach short prismatic quartz represents the first fissure mineralization. However, fluid inclusions in quartz were not observed thus we have no P-T estimate for this primary crystallization. Quartz frequently grows on fine grained seams of unspecified Ca-rich zeolites. We assume that these seams of polycrystalline zeolite are a transformation product of the host rock due to hydrothermal activity accompanied with plagioclase decomposition. Fluid inclusion measurements on bulky light green fluorite from Gibelsbach yielded a homogenization temperature for a pure H_2O fluid of ca. 160 ± 5 °C. Assuming a geothermal gradient of 30 °C/km and $P(H_2O) = P(total)$ (MULLIS, 1993), 160 °C corresponds to a depth of ca. 5–6 km equivalent to a pressure of above 1.3 kbar. Thus, a pressure correction (ca. 1 kbar) to the homogenization temperature (160 °C) becomes necessary, increasing the fluid temperature above

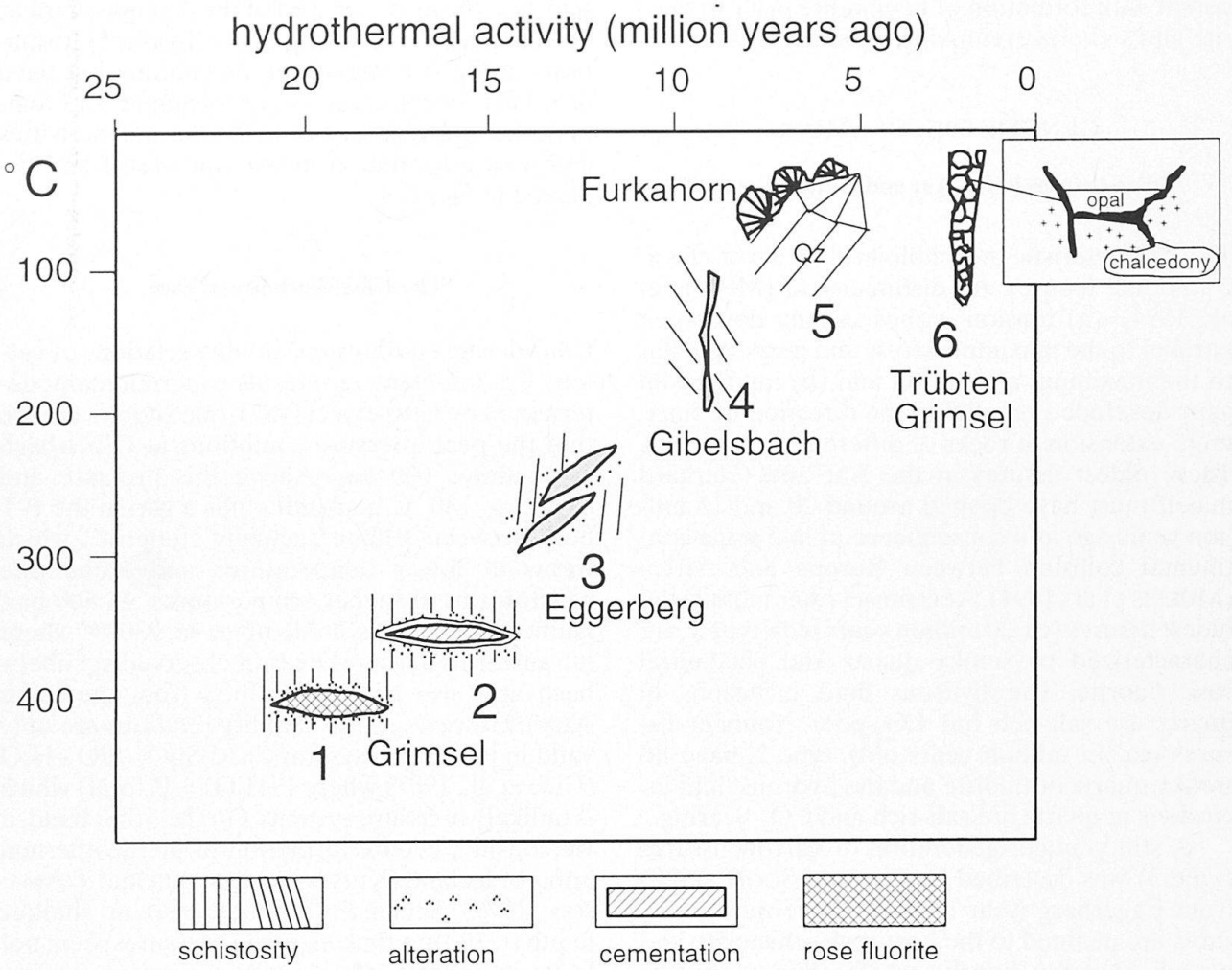

No.	description	fluid incl.	host rock	fluorite	SiO_2
1	normal Alpine fissures ca. perpendicular to penetrative schistosity	H_2O, salt-rich CO_2-poor Na >> Ca	strong alteration (dissolution) hardly cementation	octahedra rose	smoky quartz, quartz with sutures
2	as 1	H_2O, salt-rich CO_2-bearing Na >> Ca	pronounced alteration cementation (Fe-carbonate, mica)	absent	quartz (no smoky quartz) mostly no sutures
3	narrow fissures, inclined to schistosity	?	weak alteration	dodecahedra {110} with micros. {100} steps, light green	no quartz
4	extended system of vertical narrow fissures and fractures	H_2O, salt-poor, CO_2-poor	no alteration	octahedra colorless-green	small short prismatic quartz
5	relics of young fluid transportation	?	no alteration	micro-crystalline spherulites on older fissure quartz	hyalite at other locality
6	large fracture breccia	?	no alteration	absent	chalcedony, opal, quartz

Fig. 4 Schematic representation of temperature-age relations of hydrothermal activity and fissure formations in the western part of the Aar massif (southern zone). Size relations of the individual fissure symbols are arbitrary. References for the various localities are given in the text.

200 °C. If we apply this extremely rough P,T estimate (1 kbar, 200 °C) to the age-temperature development of the Aar massif at Zinggenstock (MULLIS, 1993), we may suppose that fluorite at Gibelsbach formed ca. 10 million years ago. Following CHO et al. (1987) laumontite would be the only stable Ca-rich zeolite at this P,T condition. With decreasing P,T (erosion of the Aar massif) heulandite and stellerite become successively stable.

Chabazite is known as Ca-rich zeolite forming below 100 °C thus following MULLIS (1993) this zeolite formed less than 5 million years ago. The melting point (0 °C) of fluid inclusions in Gibelsbach fluorite suggest an almost pure water fluid. These "pure water" fluid inclusions seem to be characteristic of relatively young steeply dipping quartz fissures of the Aar and Gotthard massif (STALDER et al., 1980; POTY et al., 1974). The latter authors determined homogenization temperatures between 190 and 220 °C for water fluid inclusions in quartz from steeply dipping fissures in the Gotthard massif. At Gibelsbach, the Nd isotopic composition of fluorite F1 ($\varepsilon_{Nd} = -4.3$) is indicative for a dominantly crustal origin of the fluid and suggests that the high Sm/Nd ratio is a result of fractionation prior to crystallization. MULLIS et al. (1994) also assume overthrust metasediments as the source of fluids found in quartz inclusions of classical Alpine fissures.

Acknowledgements

This study originated from a chapter of the "Lizentiatsarbeit" by Thomas Kohler who acknowledges support by the Schweizerische Nationalfonds zur Förderung der wissenschaftlichen Forschung. The community Fiesch allowed road access to the Gibelsbach locality which is highly appreciated. Beda Hofmann (Naturhistorisches Museum Bern) kindly provided sample material from the Museum collection (samples labeled NMBE). Larryn Diamond (Minerlog. Petrograph. Institut, Universität Bern) is thanked for his help with electron microprobe analyses. Fritz Zweili (Geologisches Institut, Universität Bern) recorded the SEM pictures which is highly appreciated. An earlier version of this manuscript benefited from the constructive comments of Beda Hofmann (Bern), Mickey Gunter (Moscow, Idaho), and St. Merlino (Pisa, Italy).

References

ALBERTI, A., GALLI, E. and VEZZALINI, G. (1985): Epistilbite: an acentric zeolite with domain structure. Zeitschr. Kristallogr., 173, 257–265.

AKIZUKI, M. (1981): Origin of optical variation in chabazite. Lithos, 14, 17–21.

AKIZUKI, M. and NISHIDO, H. (1988): Epistilbite: Symmetry and twinning. Amer. Mineral., 73, 1434–1437.

ARMBRUSTER, TH. and KOHLER, TH. (1992): Re- and dehydration of laumontite: a single-crystal X-ray study at 100 K. N. Jb. Miner. Mh., 385–397.

BAU, M. and DULSKI, P. (1995): Comparative study of yttrium and rare-earth element behaviours in fluorine-rich hydrothermal fluids. Contrib. Mineral. Petrol., 119, 213–223.

BILL, H. and CALAS, G. (1978): Color centres, associated rare-earth ions and the origin of coloration in natural fluorites. Phys. Chem. Minerals, 3, 117–131.

BILL, H., SIERRO, J. and LACROIX, R. (1967): Origin of coloration in some fluorites. Amer. Mineral., 52, 1003–1008.

BURRUSS, R.C., GING, T.G., EPPINGER, R.G. and SAMSON, I.M. (1992): Laser-excited fluorescence of rare earth elements in fluorite: Initial observations with a laser Raman microprobe. Geochim. Cosmochim. Acta, 56, 2713–2723.

BURT, D.M. (1989): Compositional and phase relations among rare earth element minerals. In: LIPIN, B.R., MCKAY, G.A. (eds): Geochemistry and mineralogy of rare earth elements. Reviews in Mineralogy Vol. 21, Mineralogical Society of America, 259–307.

CHESLEY, J.T., HALLIDAY, A.N., KYSER, T.K. and SPRY, P.G. (1994): Direct dating of Mississippi Valley-type mineralization: use of Sm–Nd in fluorite. Econ. Geol., 89, 1192–1199.

CHO, M., MARUYAMA, S. and LIOU, J.G. (1987): An experimental investigation of heulandite-laumontite equilibrium at 1000 to 2000 bar P_{fluid}. Contrib. Mineral. Petrol., 97, 43–50.

CONSTANTOPOULOS, J. (1988): Fluid inclusions and rare earth element geochemistry of fluorite from south-central Idaho. Econ. Geol., 83, 626–636.

DOLLINGER, H. (1989): Petrographische und geochemische Untersuchungen des Altkristallins zwischen Nägelisgrätli und Oberaarjoch (Grimsel, Kanton Bern). Hydrothermale Veränderung granitischer Gesteine in der Grimselregion (Mittleres Aarmassiv). Lizentiatsarbeit, Mineralogisch-petrographisches Institut, Universität Bern, 175 p.

EKAMBARAM, V., BROOKINS, D.G., ROSENBERG, P.E. and EMANUEL, K.M. (1986): Rare-earth element geochemistry of fluorite-carbonate deposits in western Montana, U.S.A. Chem. Geol., 54, 319–331.

FLEISCHER, M. (1969): The lanthanide elements in fluorite. Indian Mineral., 10, 36–39.

GALLI, E. and ALBERTI, A. (1975): The crystal structure of stellerite. Bull. Soc. Franc. Miner. Crist., 98, 11–18.

GALLI, E. and RINALDI, R. (1974): The crystal chemistry of epistilbites. Amer. Mineral., 59, 1055–1061.

GOETZINGER, M.A. and KOSS, S. (1995): Zum Fluorit. Mineralienwelt, 6, 26–32.

GOETZINGER, M.A. and WEINKE, H.H. (1984): Spurenelementgehalte und Entstehung von Fluoritmineralisationen in den Gutensteiner Schichten (Anis – Mitteltrias), Nördliche Kalkalpen, Österreich. Tschermaks Miner. Petrogr. Mitt., 33, 101–119.

GOTTARDI, G. and GALLI, E. (1985): Natural Zeolites, Springer Verlag.

GOTTARDI, G. (1979): Topologic symmetry and real symmetry in framework silicates. Tschermaks Miner. Petrogr. Mitt., 26, 39–50.

HINTZE, C. (1897): Handbuch der Mineralogie. Vol. 2 (Silikate und Titanate). Von Veit, Leipzig.

KENNGOTT, A. (1866): Die Mineralien der Schweiz nach ihren Eigenschaften und Fundorten ausführlich beschrieben. Verlag W. Engelmann, Leipzig.

KOENIGSBERGER, J. (1940): Die zentralalpinen Mineral-lagerstätten. In: Die Mineralien der Schweizer Alpen, Band 2, 309–501. Verlag Wepf & Co., Basel.

KOHLER, TH. (1993): Ca-reiche Zeolithe: Entwässerung des Laumontits und Kationenaustausch am Heulandit. Lizentiatsarbeit, Mineralogisch-petrographisches Institut, Universität Bern, 120 Seiten.

KRISTANNSDOTTIR, H. and TOMASSON, J. (1978): Zeolite zones in geothermal areas in Iceland. In: SAND, L.B. and MUMPTON, F.A. (eds): Natural Zeolites: Occurrence, Properties, Use. Pergamon Press, 277–284.

KÜRSTEINER, P. and SOOM, M. (1986): Chobelwand-Fluoritfundstelle im Alpstein. Schweizer Strahler, 7, 205–219.

LEEDER, O. (1966): Geochemie der seltenen Erden in natürlichen Fluoriten und Kalziten. Freib. Forschungsh., 206, 1–137.

LIEBER, W. (1995): Farbentstehung und Verteilung in Fluorit. Aufschluss, 46, 1–11.

MARCHAND, L., JOSEPH, D., TOURAY, J.C. and TREUIL, M. (1976): Critères d'analyse géochimique des gisements de fluorine basés à la distribution des lanthanides – application au gîte de Maine (71 – Cordesse, France). Mineral. Deposita, 11, 357–379.

MASUDA, A., NAKAMURA, N. and TANAKA, T. (1973): Fine structures of mutually normalized rare-earth patterns of chondrites. Geochim. Cosmochim. Acta, 37, 239–248.

MAZZI, F. and GALLI, E. (1983): The tetrahedral framework of chabazite. N. Jb. Mineral. Mh., 1983, 461–480.

MEIER, W.M. and OLSON, D.H. (1992): Atlas of zeolite structure types. Zeolites, 12, 449–654.

MERKLE, A.B. and SLAUGHTER, M. (1968): Determination and refinement of the structure of heulandite. Amer. Mineral., 53, 1120–1138.

MOELLER, P., PAREKH, P.P. and SCHNEIDER, H.J. (1976): The application of Tb/Ca–Tb/La abundance ratios to problems of fluorspar genesis. Mineral. Deposita, 11, 111–116.

MORGAN, J.W. and WANDLESS, G.A. (1980): Rare earth elements in some hydrothermal minerals: evidence for crystallographic control. Geochim. Cosmochim. Acta, 44, 973–980.

MULLIS, J. (1993): Die Entstehung alpiner Klüfte und Kluftmineralien. Lapis, 5, 17–32.

MULLIS, J., DUBESSY, J., POTY, B. and O'NEIL, J. (1994): Fluid regimes during late stages of a continental collision: Physical, chemical, and stable isotope measurements of fluid inclusions in fissure quartz from a geotraverse through the Central Alps, Switzerland. Geochim. Cosmochim. Acta, 58, 2239–2267.

NÄGLER, TH.F., PETTKE, TH. and MARSHALL, D. (in press): Initial isotopic heterogenity and secondary disturbance of the Sm–Nd system in fluorites: A study on mesothermal veins from the central and western Swiss Alps. Chem. Geol. (Isotope Geosci. Sect.).

NIGGLI, P. (1940): Zur Entstehungsgeschichte der alpinen Kluftminerallagerstätten. In: Die Mineralien der Schweizer Alpen, Band 2, 505–627. Verlag Wepf & Co., Basel.

OBENAUER, K. (1933): Zur Tracht und Paragenese des Flussspats. N. Jb. Min. Geol. Pal., 66, Abt. A, 89–119.

OGI, H. and SOOM, M. (1988): Eine Winterfundstelle: Fluorit und andere Mineralien von Eggerberg (Lötschberg-Südrampe, VS). Schweizer Strahler, 8, 153–166.

PARKER, R.L. (1973): Die Mineralfunde der Schweiz. Neuberarbeitung durch STALDER, H.A., DE QUERVAIN, F., NIGGLI, E., GRAESER, S., Verlag Wepf & Co., Basel.

PASSAGLIA, E., GALLI, E., LEONI, L. and ROSSI, G. (1978): The crystal chemistry of stilbites and stellerites. Bull. Minéral., 101, 368–375.

POTY, B.P., STALDER, H.A. and WEISBROD, A.M. (1974): Fluid inclusion studies in quartz from fissures of Western and Central Alps. Schweiz. Mineral. Petrogr. Mitt., 54, 717–752.

ROSE, G. (1826): Über den Epistilbit, eine neue zur Familie der Zeolithe gehörige Mineralgattung. Ann. Phys. Chem., Leipzig, 6, 183–189.

RYKART, R., FREI, W. and WUERSCH, D. (1983): Grüner Fluorit aus Quarzgängen im Nufenengebiet. Schweiz. Strahler, 6, 307–311.

RYKART, R. and HOTZ, K. (1987): Hyalit als jüngste Mineralbildung in einer alpinen Zerrkluft. Schweizer. Strahler, 7, 541–545.

SCHALTEGGER, U. and KRÄHENBÜHL, U. (1990): Heavy rare-earth element enrichment in granites of the Aar massif (Central Alps, Switzerland). Chem. Geol., 89, 49–63.

SHANNON, R.D. (1976): Revised effective ionic radii and systematic studies of interatomic distances in halides and chalcogenides. Acta. Cryst., A32, 751–767.

SPETTEL, B., NIEDERMAYER, G., PALME, H., KURAT, G. and WÄNKE, H. (1981): Spurenelemente in Fluoriten aus alpinen Klüften. Fortschr. Mineral., 59, Beiheft 1, 191–192.

STALDER, H.A. (1964): Petrographische und mineralogische Untersuchungen im Grimselgebiet (Mittleres Aarmassiv). Schweiz. Mineral. Petrogr. Mitt., 44, 187–398.

STALDER, H.A., SICHER, V., LUSSMANN, L. and SCHENKER, F. (1980): Die Mineralien des Gotthardbahn- und des Gotthardstrassen-Tunnels. Repof Verlag, Gurtnellen.

STALDER, H.A. (1986): Beschreibung der geschützten Kluft Gerstenegg, Grimsel, Bericht Naturschutzinspektorat Kanton Bern, Mitt. Naturforsch. Ges. Bern, 43, 41–60.

TAYLOR, S.R. and MCLENNAN, S.M. (1985): The continental crust: its composition and evolution. Blackwell, Oxford.

TRINKLER, M., KEMPF, U., PLOETZE, M. and RIESER, U. (1993): Über rosa und braunen Fluorit aus Sn-W-Lagerstätten. Chem. Erde, 53, 165–181.

TSCHERNICH, R.W. (1992): Zeolites of the World. Geosciene Press Inc., Phoenix Arizona.

VON FELLENBERG, E. (1891): Über den Flussspath von Oltschenalp und dessen technische Verwertung. Mitt. Naturforsch. Ges. Bern, 202–219.

WALKER, J.B. and CHOPPIN, G.R. (1967): Thermodynamic parameters of fluoride complexes of the lanthanides. Adv. Chem., 71, 127–140.

WISER, D.F. (1860): Krystallographische Mitteilungen. Neues Jahrb. Miner. Geogn. Geolog. 784–787.

YANG, P. and ARMBRUSTER, TH. (1996): (010) disorder, partial Si,Al ordering and Ca distribution in triclinic (C1) epistilbite. Eur. J. Mineral. 8, 263–271.

ZBINDEN, P. (1949): Geologisch-petrographische Untersuchungen im Bereich südlicher Gneise des Aarmassivs (Oberwallis). Schweiz. Mineral. Petrogr. Mitt. 29, 221–356.

Manuscript received November 24, 1995; minor revision accepted February 13, 1996.